Supplementary Data for:

Title of article: Role of Cytosolic, Tyrosine-Insensitive Prephenate Dehydrogenase in *Medicago truncatula*

Authors: Craig A. Schenck[1,2], Josh Westphal[1], Dhileepkumar Jayaraman[3], Kevin Garcia[3,4], Jiangqi Wen[5], Kirankumar S. Mysore[5] Jean-Michel Ané[3,6], Lloyd W. Sumner[7,8] and Hiroshi A. Maeda[1,*]

Affiliations: [1]Department of Botany, University of Wisconsin-Madison, Madison, WI 53706
[2] Current address: Department Biochemistry and Molecular Biology, Michigan State University, East Lansing, MI 48824
[3] Department of Bacteriology, University of Wisconsin-Madison, Madison, WI 53706
[4] Department of Crop and Soil Sciences, North Carolina State University, Raleigh, NC 27695
[5] Noble Research Institute, LLC., Ardmore, OK, USA
[6] Department of Agronomy, University of Wisconsin-Madison, Madison, WI 53706
[7] Department of Biochemistry, University of Missouri, Columbia, MO 65211
[8] Metabolomics and Bond Life Sciences Centers, University of Missouri, Colubmia, MO 65211

[*]Corresponding author: Hiroshi A. Maeda (maeda2@wisc.edu)

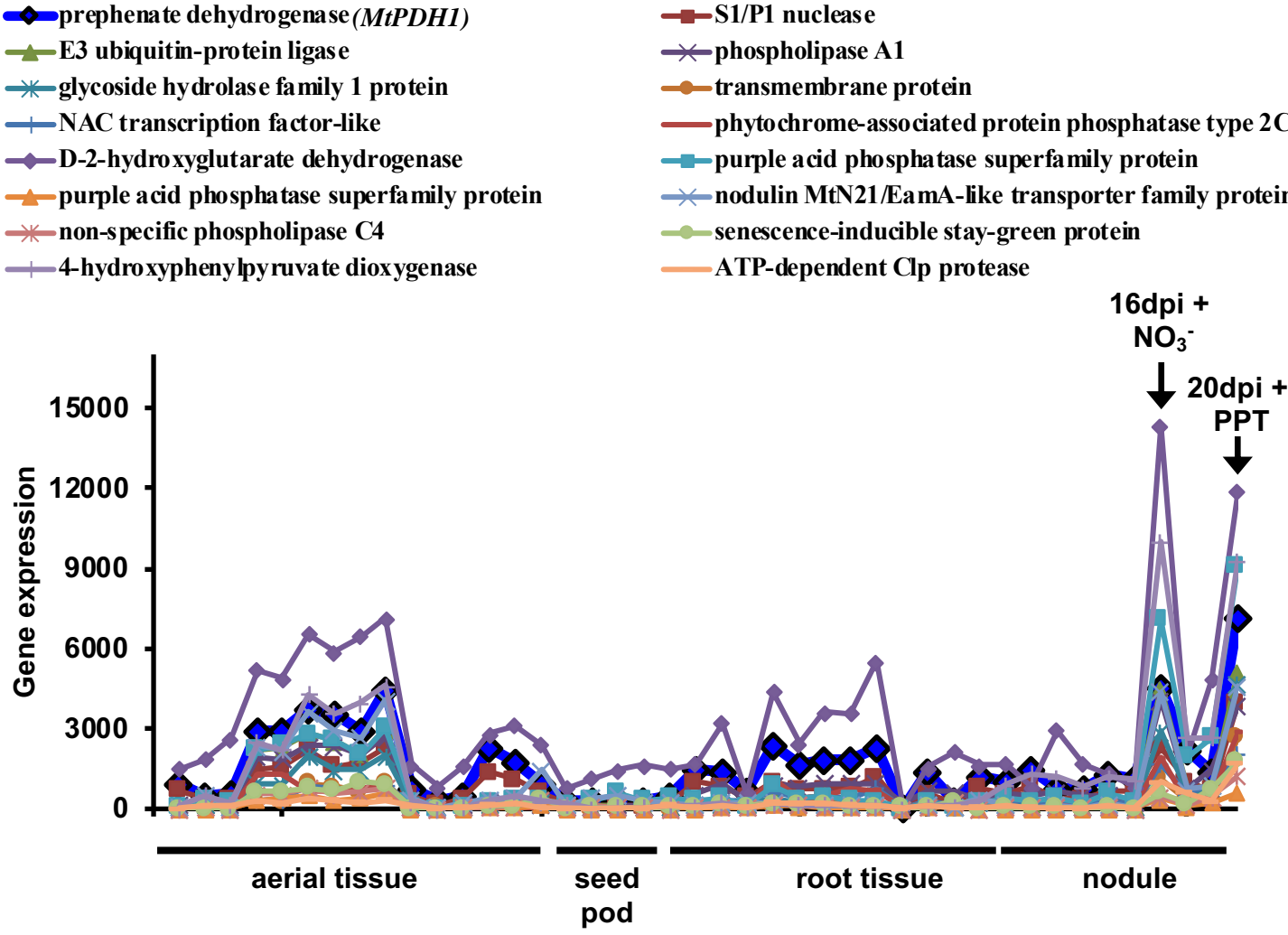

Supplementary Figure 1. Co-expression analysis of *MtPDH*. Co-expressed genes with *MtPDH1* were identified in various tissue-types and treatments using the Medicago gene expression atlas (www.mtgea.noble.org/v3/) with a Pearson's correlation coefficient of > 0.7. *MtPDH1* (blue line with square symbols) was co-expressed with senescence related genes, including proteases, lipases as well as HPP dioxygenase (HPPD), which catalyzes the initial step in Tyr catabolism. Additionally, *MtPDH1* was induced under two nodule conditions, highlighted by black arrows, that likely trigger senescence related processes, 16 dpi + nitrate (NO_3^- Benedito et al., 2008) and 20 dpi + Phosphinothricin (PPT) treatment (Seabra et al., 2012).

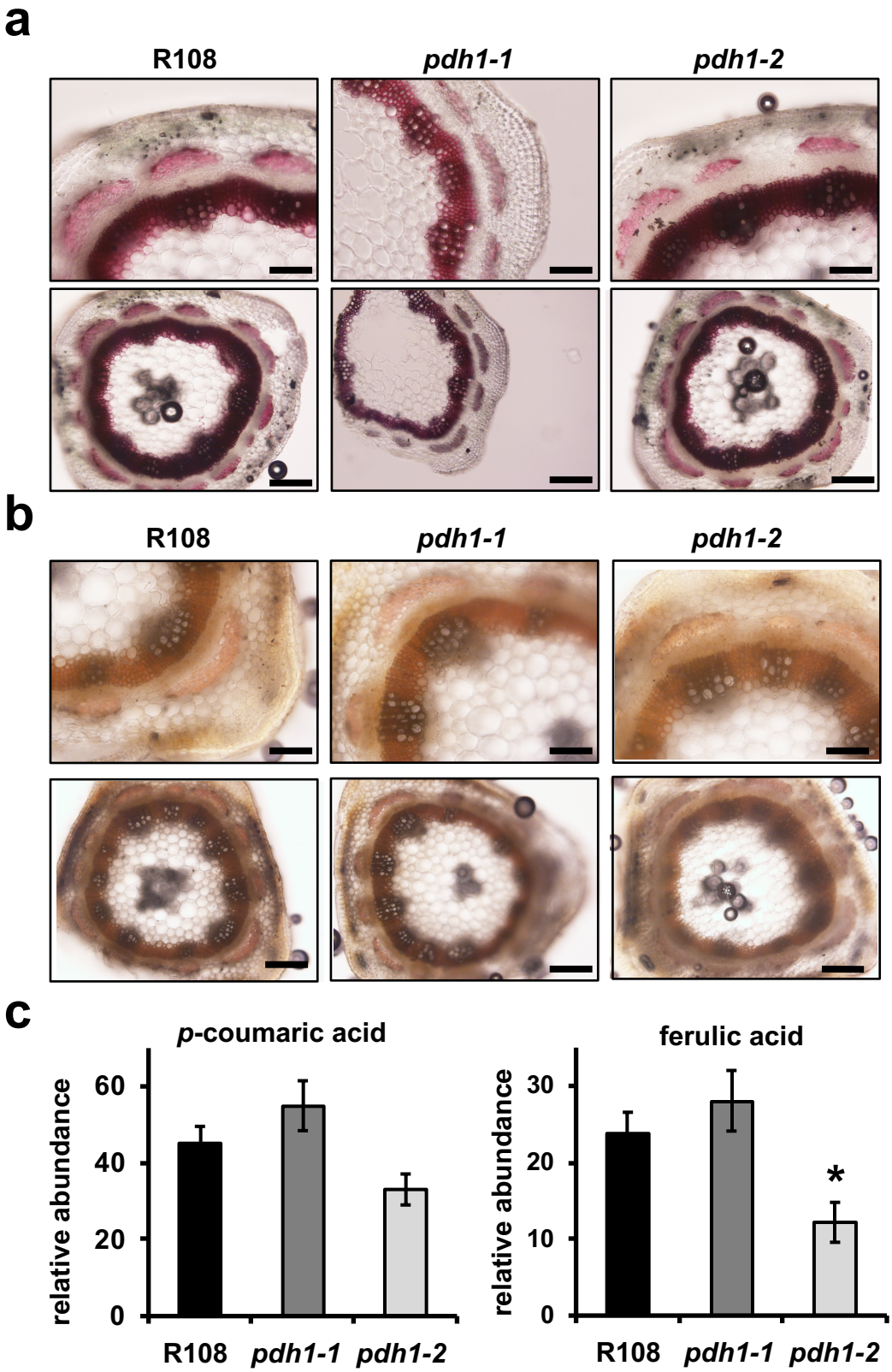

Supplementary Figure 2. Effects of PDH pathway mutations on Phe-derived metabolism. Lignin composition and linkages were assessed in Wt (R108) and mutants using two histochemical stains **(a)** phloroglucinol, and **(b)** Mäule staining. The top panel is 10x magnification (scale bars 50 μm), bottom panel is 4x magnification (scale bars 125 μm). Equal staining was observed in mutants compared with Wt (R108). **(c)** Phenylpropanoid compounds that serve as lignin precursors measured using GC-MS. Bars represent average metabolite abundance ± s.e.m of n ≥ 3 biological replicates. Significant differences to Wt control are indicated; *$P \leq 0.05$.

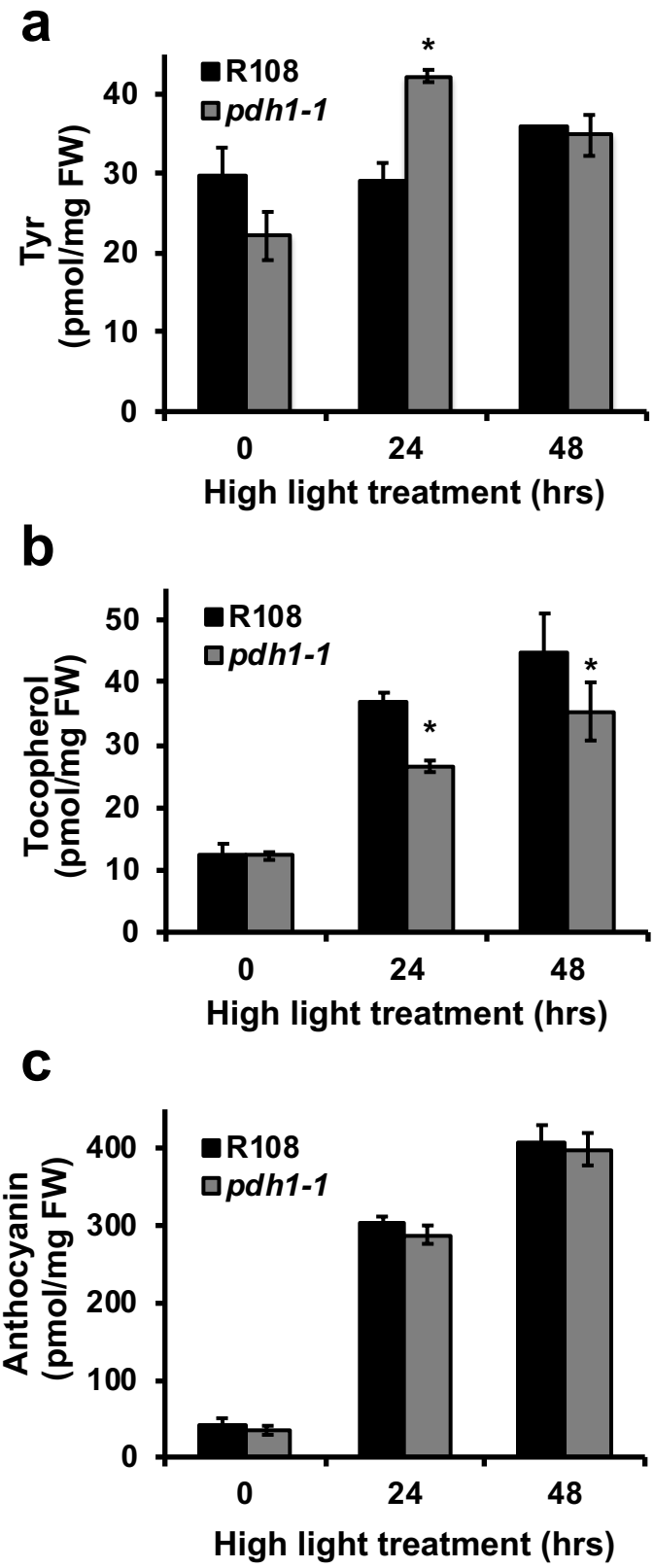

Supplementary Figure 3. High light treatment stimulates Tyr- and Phe-derived metabolism. Whole plants were moved from standard light (~200 µE) to high light (~950 µE) conditions and leaves from Wt (R108, black) and *pdh1-1* (gray) were collected after 0, 24, and 48hrs. Metabolites were extracted and identified using HPLC (Tyr and tocopherols) or spectrophotometrically (anthocyanins). Absolute quantification of Tyr **(a)**, tocopherols **(b)**, and anthocyanins **(c)** are shown as the average pmol/mg FW ± s.e.m of n = 3 biological replicates. Significant differences from the Wt (R108) control at the respective timepoints are indicated; *$P \leq 0.05$.

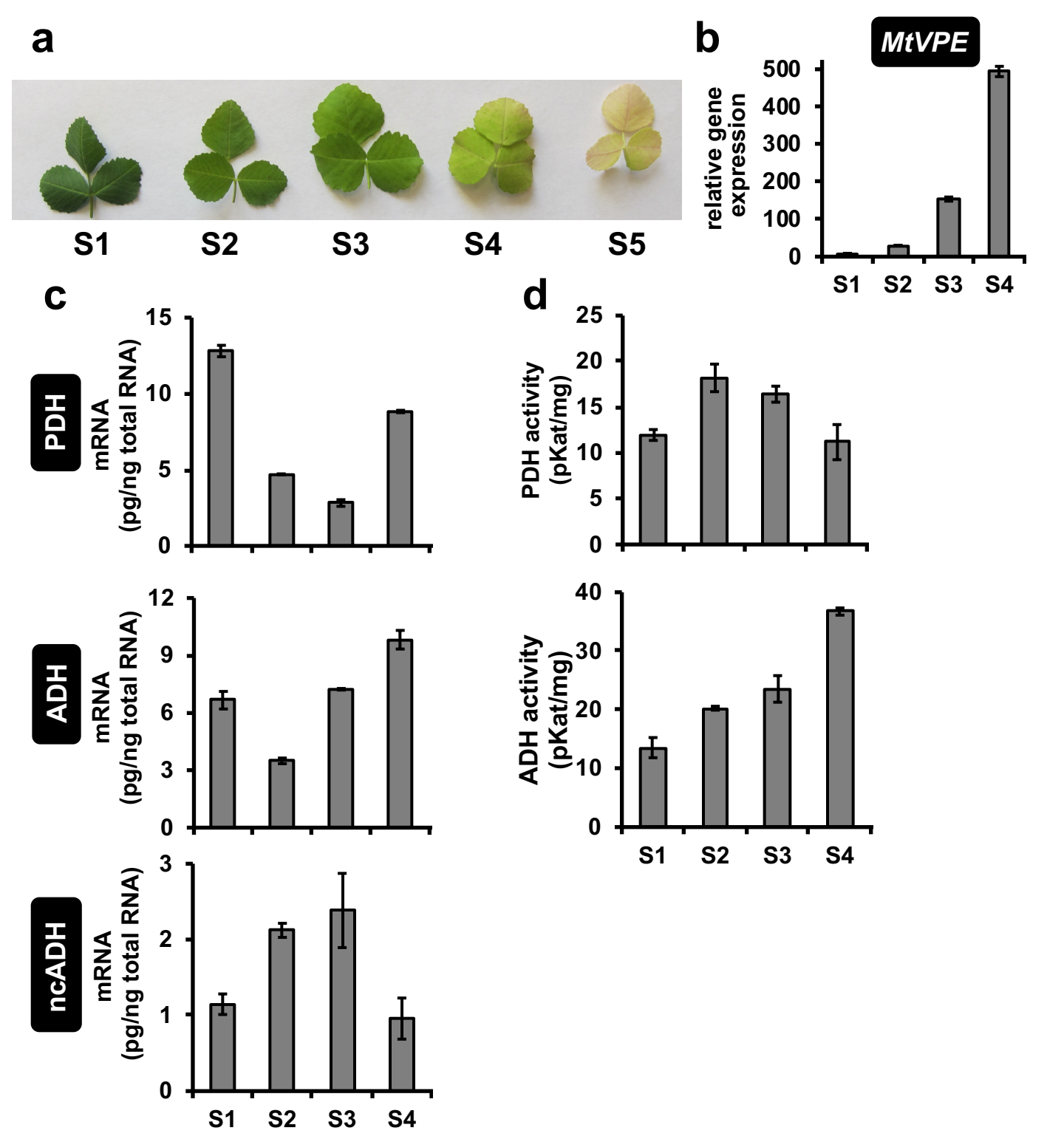

Supplementary Figure 4. PDH and ADH gene expression and enzymatic activity in senescing leaves. (a) Representative developmental time series of senescing Wt (R108) leaves used for gene expression **(b,c)** and enzymatic activity **(d)** analyses. High quality RNA and enzymes were obtained for all developmental stages except for S5. **(b)** A senescent marker gene (vacuolar processing enzyme, *MtVPE* Medtr1g016780, Pérez Guerra et al., 2010), was used as a control for qRT-PCR. Bars are average mRNA abundance ± s.e.m. of n = 3 biological replicates. **(c)** qRT-PCR analysis of *PDH* and *ADH* expression in senescing leaves, bars represent absolute mRNA abundance (pg/ng total RNA) ± s.e.m. of n = 3 biological replicates. **(d)** PDH and ADH enzymatic activity from senescing leaves. Bars represent average enzymatic activity (pKat/mg) ± s.e.m. of n = 3 biological replicates.

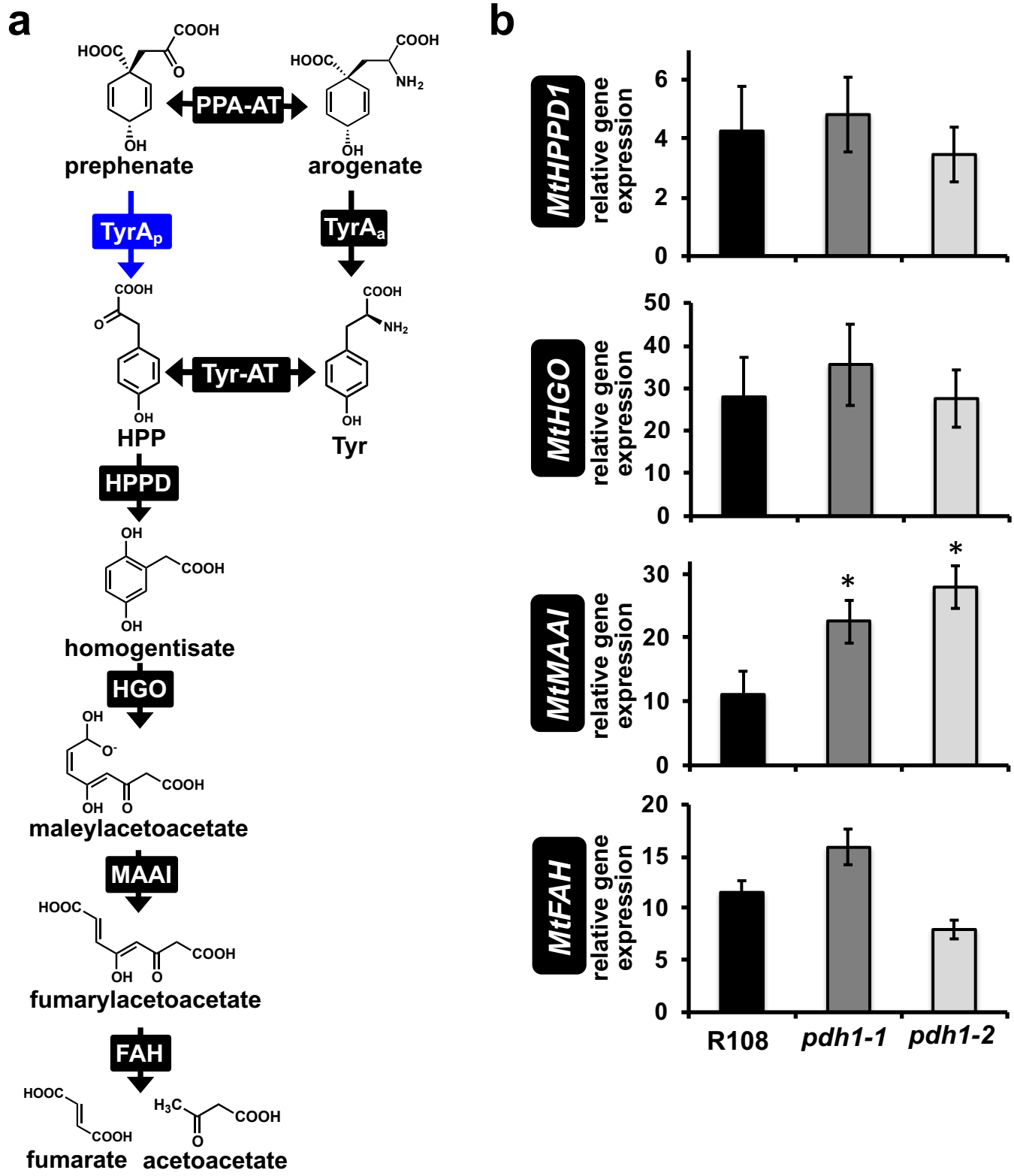

Supplementary Figure 5. Tyr degradation pathway and gene expression in PDH mutants. (a) The canonical Tyr catabolism pathway in plants. PDH (blue) provides a direct route to HPP and the Tyr catabolic pathway avoiding three ADH pathway steps (PPA-AT, TyrA$_a$, and Tyr-AT). **(b)** Gene expression analysis of Tyr catabolic pathway enzymes from RNA extracted from six week old leaf tissue from Wt (R108) and *mtpdh1* mutants. Bars represent average gene expression normalized to a housekeeping gene (*MtPI4K)* ± s.e.m. of n = 3 biological replicates. Significant differences to Wt (R108) control are indicated; *$P \leq 0.05$. FAH, fumarylacetoacetate hydrolase; HGO, homogentisate 1,2-dioxygenase; HPPD, HPP dioxygenase; MAAI, maleylacetoacetate isomerase; TyrA$_a$, arogenate dehydrogenase; TyrA$_p$, prephenate dehydrogenase; Tyr-AT; Tyr-aminotransferase.

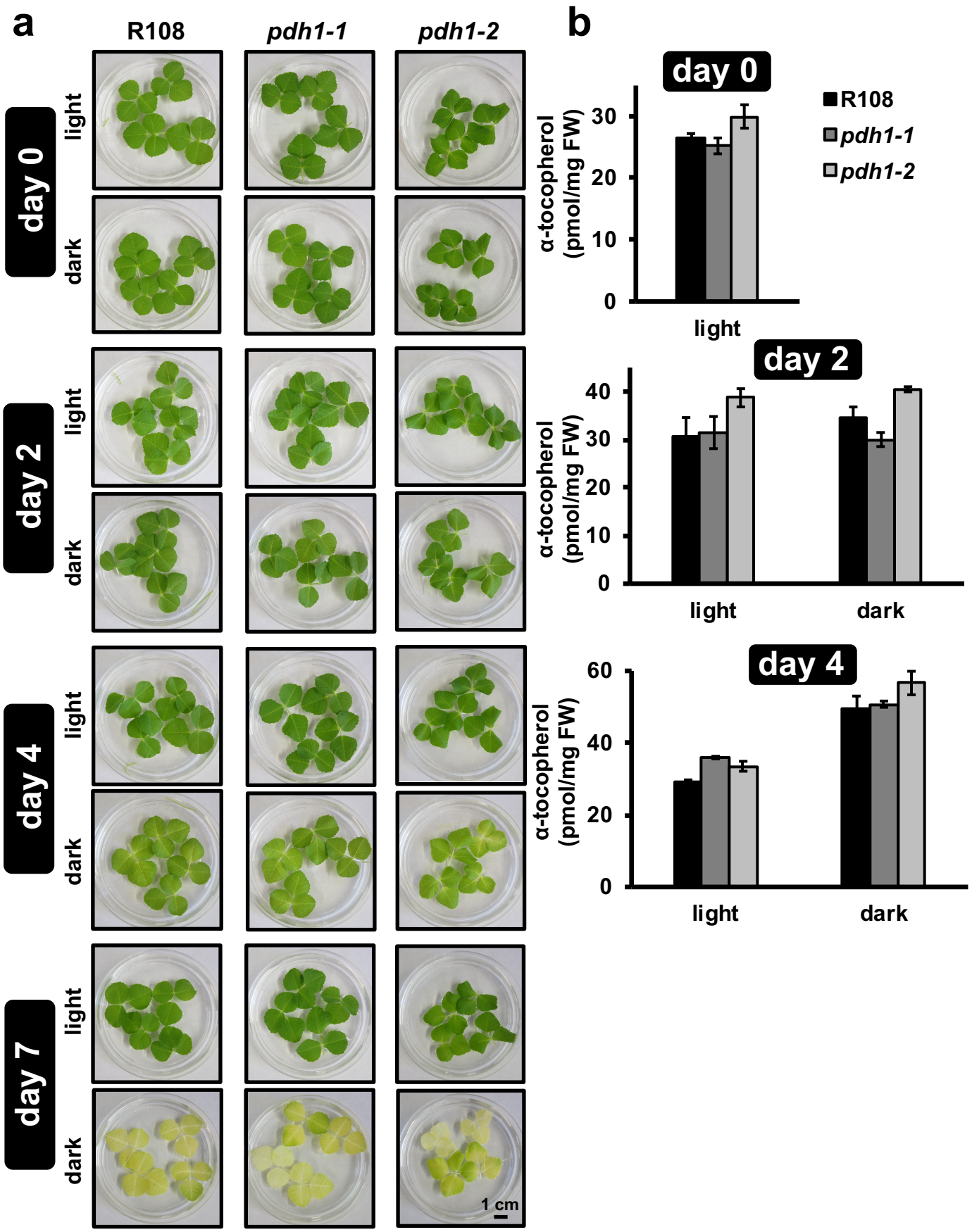

Supplementary Figure 6. Dark-induced senescence leads to accumulation of tocopherols. (**a**) Excised leaves from six week old Wt and *mtpdh1* mutants were floated on H_20 and treated in the dark, or left under normal light conditions for seven days. Dark-induced senescence progressed equally for Wt (R108) and mutants. (**b**) α-tocopherol content measured from leaves during the dark treatment expressed in pmol/mg FW ± s.e.m. of n = 3 biological replicates.

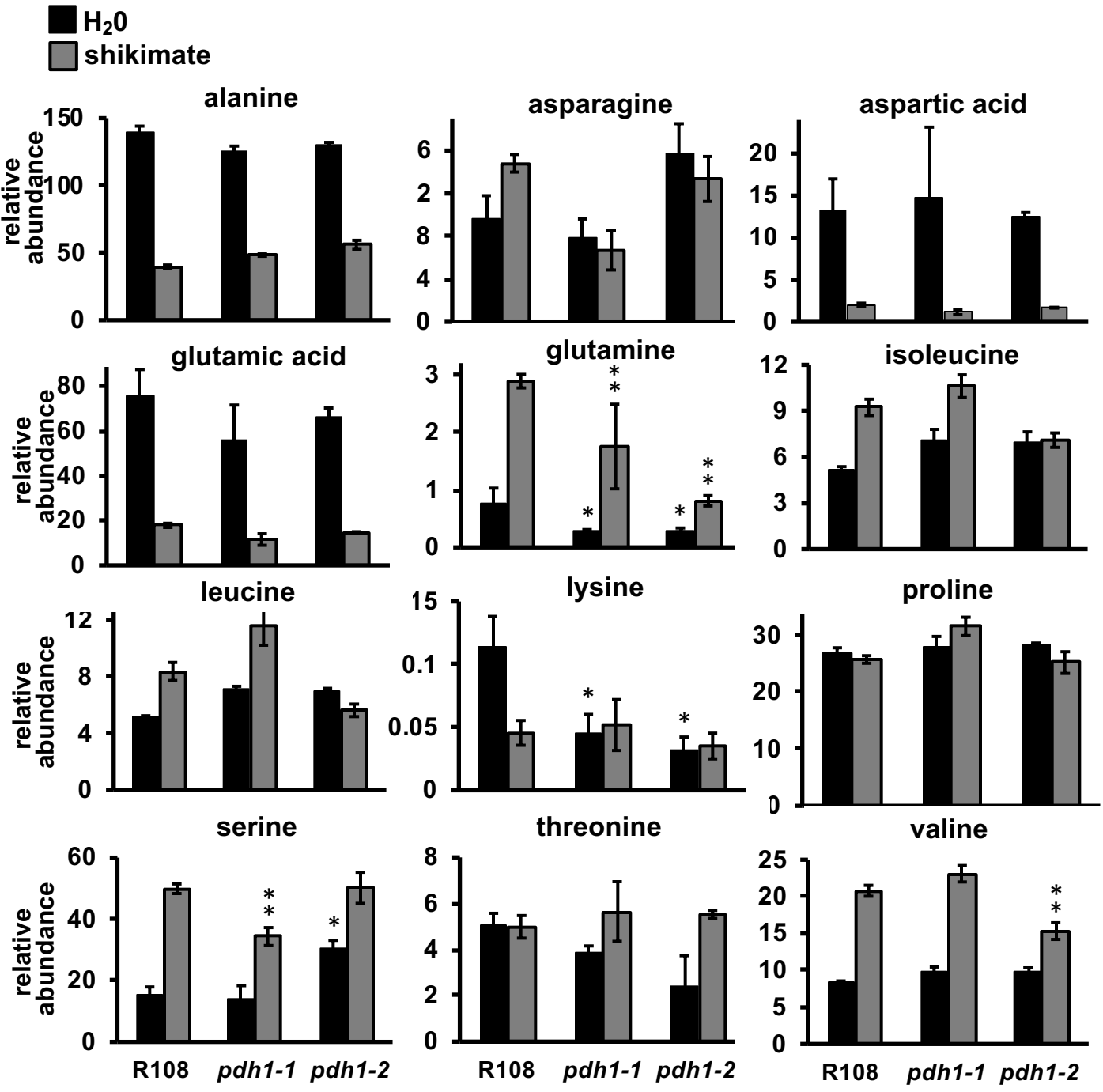

Supplementary Figure 7. Additional amino acids from shikimate feeding in Wt and mutants. Excised leaves from six week old plants were floated on H_20 (black bars) or a solution of 25 mM shikimate (Tyr precursor) (gray bars) for eight hours. Leaves were then used for metabolite extraction and identification using GC-MS. Relative abundance of the corresponding metabolites are the average ± s.e.m of n = 3 biological replicates. Significant differences from the water fed control (R108, black) are indicated; *$P \leq 0.05$, significant differences from the shikimate fed control (R108 gray) are indicated **$P \leq 0.05$.

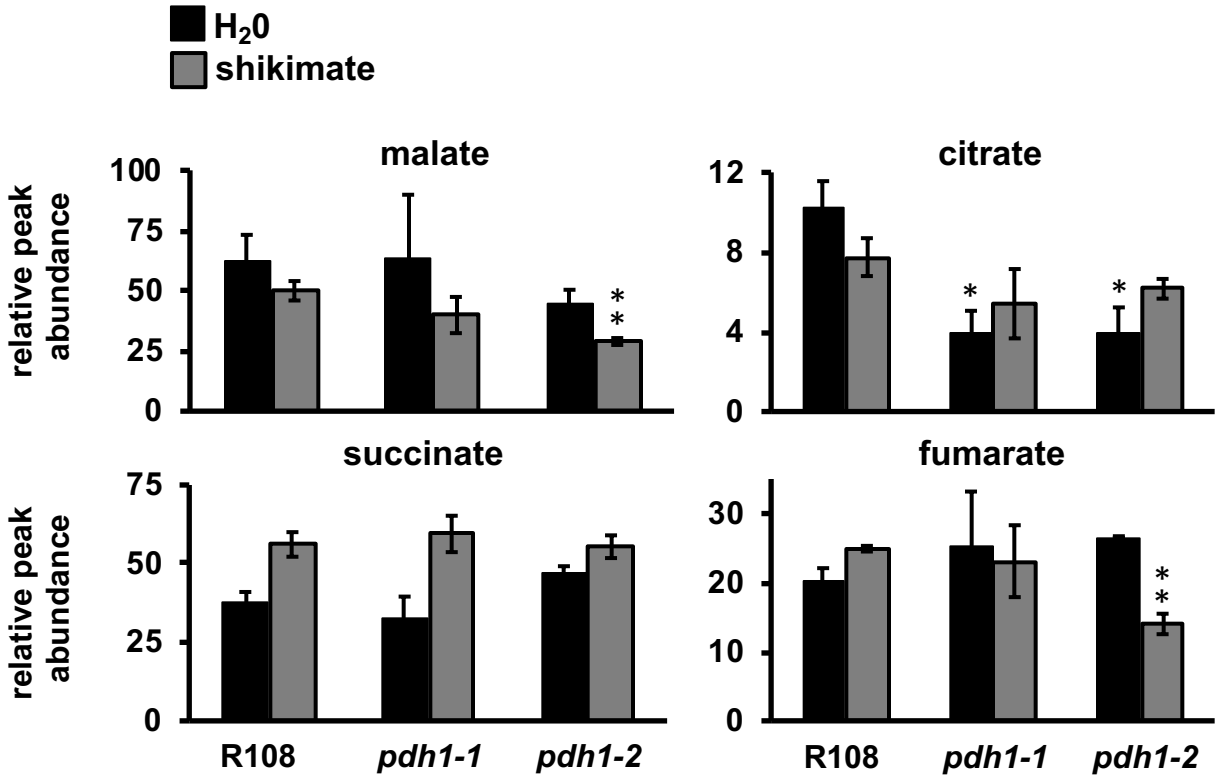

Supplementary Figure 8. TCA metabolite levels following shikimate feeding in Wt and mutants. Excised leaves from six week old plants were floated on H_20 (black bars) or a solution of 25 mM shikimate (Tyr precursor) (gray bars) for eight hours. Leaves were then used for metabolite extraction and identification using GC-MS. Relative abundance the corresponding metabolites are the average ± s.e.m of n = 3 biological replicates. Significant differences from the water fed control (R108, black) are indicated; $*P \leq 0.05$, significant differences from the shikimate fed control (R108 gray) are indicated $**P \leq 0.05$.

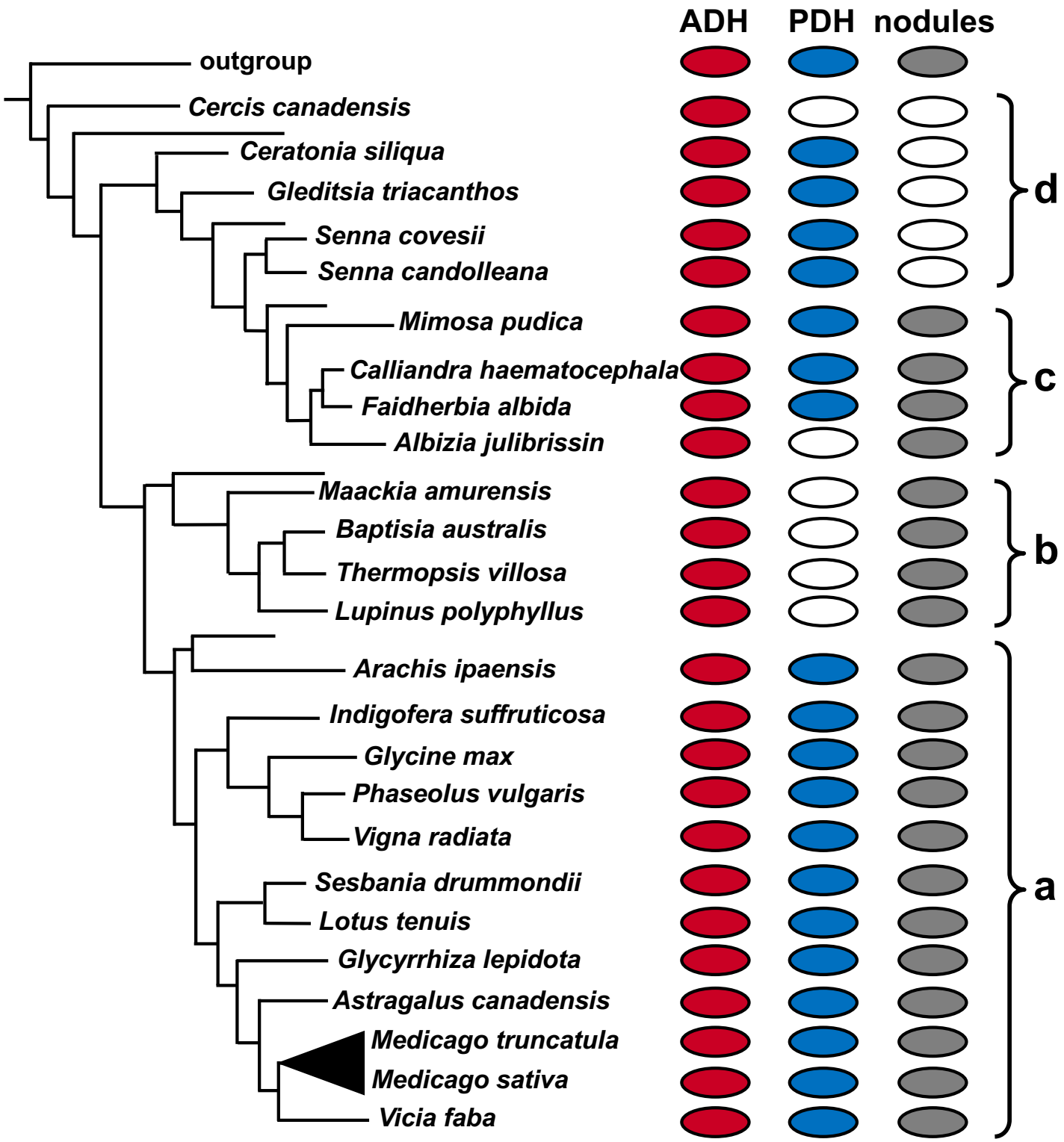

Supplemental Figure 9. Phylogenetic distribution of ADH and PDH activity and nodulation status across the Leguminosae family. ADH and PDH activities were assayed in various legume species, including **(a)** a clade containing many crop legumes, **(b)** genistoid crown clade, **(c)** mimosoid crown clade, and **(d)** early diverging lineages. They are mapped onto a representative phylogeny of Leguminoseae (Azani et al., 2017). Filled circles with red and blue colors indicate the presence of ADH and PDH activity, respectively, whereas empty circles represent the absence of enzymatic activity. Filled circles with gray denote legumes that form nodules, whereas empty circles represent legumes that do not form nodules, based on Afkhami et al. (2018).

Supplementary Table 1. Non-targeted metabolite analysis from leaf tissue of Wt and *mtpdh1-1*

Metabolite	retention time (min)	Ion (m/z)	pdh1-1/R108	pdh1-2/R108	T-test pdh1-1:R108	T-test pdh1-2:R108
Beta-Alanine	21.5809	248.1	NS	1.49638	NS	0.04629
beta-D-glucoside	32.1517	204.1	1.18350	2.20999	0.01116	0.00016
Citric Acid	30.5877	273.1	NS	1.51560	NS	0.00027
D-(+)-Melibiose	43.5201	204.1	0.72128	NS	0.03323	NS
Ferulic Acid	36.1830	338.2	NS	0.51230	NS	0.01121
Gentisic Acid	29.4116	355.2	NS	2.85714	NS	0.00001
Glucuronic Acid	29.1234	292.2	NS	1.58440	NS	0.00001
Glycolic Acid	11.8422	205.1	1.42874	1.92904	0.01487	0.00037
L-Alanine	19.8168	188.1	NS	2.39806	NS	0.00005
Lauryl Alcohol	22.0027	243.1	1.27167	NS	0.01445	NS
Maleic Acid	18.2630	2455.0	NS	0.68722	NS	0.04895
Malic Acid	23.0106	233.1	NS	0.73291	NS	0.04836
Malonic Acid	15.4680	233.1	0.75424	NS	0.02370	NS
Pinitol	30.8088	260.2	1.33875	NS	0.01147	NS
Propionic Acid	18.8585	292.2	NS	2.08458	NS	0.01253
Saccharic Acid	35.0341	333.2	0.74697	1.32846	0.00476	0.00815
Sucrose	44.9165	361.2	NS	1.99803	NS	0.02979
Tartaric Acid	25.6516	305.2	1.43056	NS	0.03744	NS
Trehalose	43.9602	361.2	NS	18.99309	NS	0.00048
Tyramine	32.7431	174.1	NS	0.59383	NS	0.00075
Unknown	33.6590	204.1	1.26433	NS	0.00363	NS
Unknown	17.5759	186.0	1.79713	2.62694	0.00452	0.01497
Unknown	13.6890	220.1	1.41853	NS	0.00884	NS
Unknown	30.8657	217.1	1.32711	NS	0.00953	NS
Unknown	9.2975	184.1	1.52453	NS	0.01137	NS
Unknown	47.8363	204.2	1.43690	1.35843	0.01504	0.04118
Unknown	47.2028	204.1	1.21975	1.20442	0.03006	0.04871
Unknown	32.5721	221.2	1.21109	NS	0.03112	NS
Unknown	49.3385	217.1	1.31458	1.40117	0.03151	0.01702
Unknown	36.3824	434.3	0.70531	NS	0.03570	NS
Unknown	21.0322	189.1	1.20140	NS	0.04070	NS
Unknown	23.6949	217.1	NS	3.31769	NS	0.00007
Unknown	32.7980	205.1	NS	3.21406	NS	0.00002
Unknown	27.4875	422.2	NS	3.08602	NS	0.01943
Unknown	17.5759	186.0	NS	2.48604	NS	0.01419
Unknown	24.6017	217.1	NS	2.38962	NS	0.00001

Unknown	22.0509	307.2	NS	2.33226	NS	0.00220
Unknown	19.1101	184.1	NS	2.02055	NS	0.04568
Unknown	30.6073	150.1	NS	1.50572	NS	0.00020
Unknown	24.9767	313.3	NS	1.43477	NS	0.04725
Unknown	31.7135	275.2	NS	1.31801	NS	0.00069
Unknown	38.4361	331.1	NS	1.27114	NS	0.00650
Unknown	33.7685	270.2	NS	0.76019	NS	0.03895
Unknown	41.0710	274.1	NS	0.70608	NS	0.01860
Unknown	37.2316	204.1	NS	0.67959	NS	0.02484
Unknown	25.7858	331.2	NS	0.65537	NS	0.01841
Unknown	31.0367	292.2	NS	0.54155	NS	0.00025
Xylose	26.8968	160.1	NS	0.60672	NS	0.00493

Only compounds are shown that were significantly different from Wt with abundance > 1.2 or < 0.8 fold-change and a P-value ≤ 0.05. Ratio of average relative metabolite abundance is shown for *pdh1-1* and *pdh1-2* compared with Wt with N = 5. NS, not significant. Unknowns are compounds that were detected with unique ions, but did not have a confident library match (< 75%).

Supplementary Table 2. Primer sequences used in this study

Name	Use	Sequence (5'-3')
PDH1-1	*mtpdh1-1* genotyping	GAGCACTATTTCCATTGTTAAC
Tnt1R	*mtpdh1-1* genotyping	CAGTGAACGAGCAGAACCTG
PDH1-2	*mtpdh1-2* genotyping	ATGAGACTGGAGGGGGAGAT
Tnt1F	*mtpdh1-1* genotyping	GAACATATGGCAGGGGTTACAAG
MtPDHqF1	*mtpdh1-1* qPCR	AAACAAGGTCATACTCTAACTGCAA
MtPDHqR1	*mtpdh1-1* qPCR	CAGCATCAAGGAATGCTGTAA
MtPDHqF2	*mtpdh1-2* qPCR	CAACAGATTCGCCAGACAAGAGC
MtPDHqR2	*mtpdh1-2* qPCR	CTGGGTTCTGTCCTTCATCGA
MtADHqF	*MtADH* (Medtr4g115980) qPCR	GACCTGAGAGTGGAAGCAGT
MtADHqR	*MtADH* (Medtr4g115980) qPCR	TTCTCACACCTCGAAACCCT
MtncADHqF	*MtncADH*(Medtr5g083530) qPCR	GCTAGTGAGGGTTGTAAGATGC
MtncADHqR	*MtncADH*(Medtr5g083530) qPCR	GCGGGTAATTCTGTATTATT
MtPI4KF[1]	housekeeping gene (*MtPI4K) qPCR*	GCAGATAGACACGCTGGGA
MtPI4KR[1]	housekeeping gene (*MtPI4K) qPCR*	AACTCTTGGGCAGGCAATAA
MtHPPD1F	*MtHPPD1* (Medtr5g091060) qPCR	CCCACCAACACCACTTCTCT
MtHPPD1R	*MtHPPD1* (Medtr5g091060) qPCR	GGTGCTGGGTTACAGCATTT
MtHGOF	*MtHGO* (Medtr8g463280) qPCR	AGGCACGGGTTCCTTCTAAT
MtHGOR	*MtHGO* (Medtr8g463280) qPCR	TCAATGAAATCCGTTGGTGA
MtMAAIF	*MtMAAI* (Medtr4g134370) qPCR	CTTCCATGGGTCCAGAGTGT
MtMAAIR	*MtMAAI* (Medtr4g134370) qPCR	CCGCCATGAAAACTTCATCT
MtFAHF	*MtFAH* (Medtr2g025640) qPCR	ACTTCGGACCCACATTGAAG
MtFAHR	*MtFAH* (Medtr2g025640) qPCR	TCCACAGGTTTTCCCAGTTC
MtVPEF[2]	*MtVPE* (Medtr1g016780) qPCR	AGTTCTGCCTGTTGTGGAATGTC
MtVPER[2]	*MtVPE* (Medtr1g016780) qPCR	GGTAGCTCCTGTCTGCCAATTAC

[1] Housekeeping gene (Kryvoruchko et al., 2016) used in normalization of qPCR data.

[2] Cysteine protease (vacuolar processing enzyme; VPE) that serves as a senescence marker gene (Pérez Guerra et al., 2010).